ADVANCED MATERIALS INTERFACES
Open Access
www.advmatinterfaces.de

Controlled Patterning of Complex Resistance Gradients in Conducting Polymers with Bipolar Electrochemistry

*Gerardo Salinas, Serena Arnaboldi, Patrick Garrigue, and Alexander Kuhn**

Conducting polymers have gained considerable attention for the possible design of localized electroactive patterns for microelectronics. In this work, the authors take advantage of the properties of polypyrrole, in synergy with a wireless polarization, triggered by bipolar electrochemistry, to produce localized resistance gradient patterns. The physicochemical modification is caused by the reduction and overoxidation of polypyrrole, which produces highly resistive regions at different positions along the conducting substrate at predefined locations. Due to the outstanding flexibility of polypyrrole, U-, S-, and E-shaped bipolar electrodes can be formed for prove-of-concept experiments, and electrochemically modified in order to generate well-defined resistance gradients. Energy-dispersive X-ray spectroscopy analysis of the samples confirms the localized physicochemical modifications. This approach presents as main advantages the wireless nature of bipolar electrochemistry and the possible fine-tuning of the spatial distribution of the electrochemical modification, in comparison with more conventional patterning methods.

1. Introduction

Conducting polymers are materials that have gained considerable attention due to their outstanding mechanical, optical, and electric properties.[1–5] These are based on the reversible transition between insulating and conducting states, triggered by a chemical or electrochemical reaction, which cause changes of the doping state of the polymer. The use of such π-conjugated materials enables different interesting applications, ranging from sensing and energy storage to environmental remediation and bioelectronics.[6–11] In particular, due to the possible fine-tuning of their conductivity, these polymers have emerged as an alternative for the design of localized electroactive patterns for microelectronics.[12,13] Different fabrication techniques are typically used in this context, such as inject-printing, photothermic patterning, 3D printing and imprinting, as well as electron-beam or UV lithography,[14–21] producing, e.g., well-defined conductivity patterns on polypyrrole and poly(3,4-ethylenedioxythiophene)/polystyrene sulfonate substrates.[16,20] However, low-cost and straightforward methods for the localized patterning of conductive substrates are highly desired. In this frame, bipolar electrochemistry (BE) is presented as an interesting alternative for the localized modification of conductive objects.[22–27] The concept is based on the asymmetric polarization of a conducting substrate due to presence of an external electric field (ε). Under such conditions, a polarization potential difference (ΔV) is generated at each extremities of the object, the bipolar electrode (BPE), which is exposed to ε in an electrolyte solution. In the presence of electroactive species, redox reactions occur at both extremities of the BPE only when ΔV exceeds the thermodynamic threshold potential (ΔV_{min}). This concept has been used for the asymmetric generation of patterned gradients, ranging from the chemical composition to the wettability of the material.[28–33] In recent years, the approach has also been used to produce gradients with organic thin films either by bipolar electrolytic micelle disruption or electrografting.[34–36] A promising alternative is to take advantage of the efficient insulator/conductor transition of conducting polymers in order to produce asymmetric charging/discharging gradients.[37] For example, Inagi et al. have used this concept to induce conductivity patterns in different π-conjugated polymers such as polyaniline, poly-3,4-dioxythiophene, poly-3-methylthiophene, and co-poly(9-fluorenol)-(9,9-dioctyfluorene) using U-shaped bipolar electrochemistry cells.[38–41] Furthermore, it has been demonstrated that by using sophisticated bipolar electrochemical setups, it is possible to generate steep localized doping gradients.[42] Herein, we take advantage of the bipolar electrochemistry approach, in order to generate localized resistance gradients on a flexible free-standing polypyrrole strip (Ppy), doped with dodecyl benzenesulfonate anions (DBS). The asymmetric modification of conducting polymers by bipolar electrochemistry has been previously reported, but mostly focusing on optical transitions (changes in color). Since for conducting polymers, conductivity

G. Salinas, P. Garrigue, A. Kuhn
University of Bordeaux
CNRS, Bordeaux, INP, ISM, UMR 5255, ENSCBP, Pessac 33607, France
E-mail: kuhn@enscbp.fr
S. Arnaboldi
Dipartimento di Chimica
Universita degli Studi di Milano
Via Golgi 19, Milano 20133, Italy

The ORCID identification number(s) for the author(s) of this article can be found under https://doi.org/10.1002/admi.202202367.

DOI: 10.1002/admi.202202367

ADVANCED MATERIALS INTERFACES
Open Access
www.advmatinterfaces.de

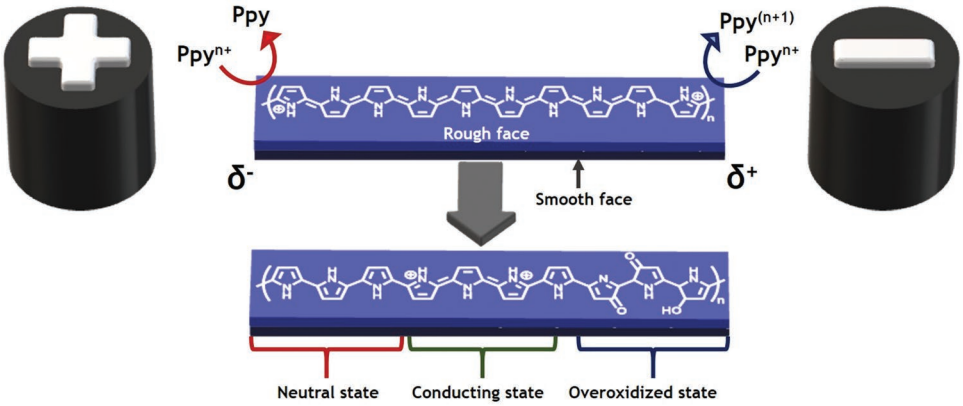

Scheme 1. Schematic illustration of the wireless modification of a charged Ppy/DBS strip placed between two feeder electrodes, before and after the asymmetric modification, with a representation of the chemical structures and the associated redox reactions.

is a bulk property, small variations of the mobility of the charge carriers result in more pronounced resistance/conductance changes, in comparison with absorbance. Thus, the proposed approach allows a fine-tuning of the local electric properties based on a simple experimental setup. By applying a high-enough electric field, the charged Ppy strip (Ppy^{n+}) experiences a respective reduction (discharge) and overoxidation (Ppy^{n+1}) at its extremities (**Scheme 1**), leading to an asymmetric increase of resistance. In addition, and most importantly, different BPE configurations were designed, just by folding the Ppy film, in order to generate localized resistance gradient patterns.

2. Results and Discussion

The Ppy substrates were synthesized galvanostatically from an aqueous solution of sodium dodecyl benzenesulfonate (DBS) and pyrrole monomer. Under these conditions, the obtained final Ppy film is in its oxidized state, with the DBS anions inside the polymer matrix to maintain electroneutrality. Due to the relative bulkiness of the anion and the compacted polymer chains, the exchange of DBS ions during the redox transitions is limited. Thus, for this system, the charging/discharging transition is accompanied by a cation release/uptake. The asymmetric modification of the free-standing Ppy/DBS strips was carried out by placing the corresponding BPE at the center of a bipolar cell containing a 5 mM $LiClO_4$ aqueous solution. First, a straight 3-cm long Ppy strip was used in order to check the formation of resistance gradients (**Figure 1**a). As stated above, under these conditions, when enough electric field is applied, overoxidation and reduction of the charged Ppy strip takes place, respectively, at the two extremities. These reactions lead to the formation of the neutral state of Ppy and overoxidized pyrrolinones units (Scheme 1).[43,44] It is important to note that during Ppy overoxidation, irreversible cross-linking of neighboring oligomeric chains may also occur. Theoretically, the ΔV_{min} required to trigger such reactions is found to be around 1.6 V,[43] thus, an ε of over 0.5 V cm^{-1} is needed to asymmetrically polarize a 3-cm Ppy strip. However, due to the potential drop at the feeder electrodes and the wireless polarization of the BPE, in comparison with a direct connection, a higher electric field is required. In the previous work, it has been demonstrated that only when an electric field of 4 V cm^{-1} is applied, it is possible to trigger such redox reactions at the extremities of a 1-cm Ppy/DBS film,[45] corresponding to a ΔV_{min} of 4 V. Thus, in order to ensure a sufficient asymmetric polarization of the BPE, the applied electric field was calculated assuming a ΔV_{min} of 6 V. A more detailed explanation concerning the calculation of the electric field is available in the Supporting Information. As it can be seen by comparing Figure 1b,c, applying a constant ε of 2 V cm^{-1} changes the resistance at each extremity of the BPE, due to the overoxidation and reduction of the pristine-doped Ppy/DBS film.

Furthermore, the resistance gradients propagate from the anodic and cathodic extremity toward the center of the strip when the time of exposure to the electric field is increased (Figure S1, Supporting Information).

After this first set of experiments, the possible generation of localized resistance gradients along the polymer was studied. This was carried out by folding the Ppy strip and placing it on a holder, in such a way that a U-shaped BPE was obtained. However, the free-standing Ppy/DBS presents two different surface morphologies: (i) a rough face, which was in contact with the solution during the galvanostatic polymerization, and (ii) a smooth face that was in direct contact with the Au substrate (Figure S2, Supporting Information). Thus, by bending the object with the smooth or rough face outwards, it is possible to obtain two different U-shaped BPE configurations. Since such an object presents an effective length of 1.5 cm with respect to the electric field, 4 V cm^{-1} is required to efficiently polarize the Ppy strip. As the extremities and the middle part of the U-shaped Ppy are facing the cathodic and anodic feeder electrodes, respectively, three different polarization regions can be produced (Figure 1d,e). As it can be seen, after the polarization, the BPE with the smooth face orientated outwards presents a resistance profile similar to the unfolded Ppy strip (Figure 1f). For the opposite configuration, using the U-shaped Ppy strip with the rough surface facing outwards, three well-defined resistance gradients are obtained at different regions along the BPE (Figure 1g). This difference between the obtained resistance gradients is due to the intrinsic anisotropy in surface roughness of the Ppy film. Each face is characterized by a resist-

ADVANCED MATERIALS INTERFACES
Open Access
www.advmatinterfaces.de

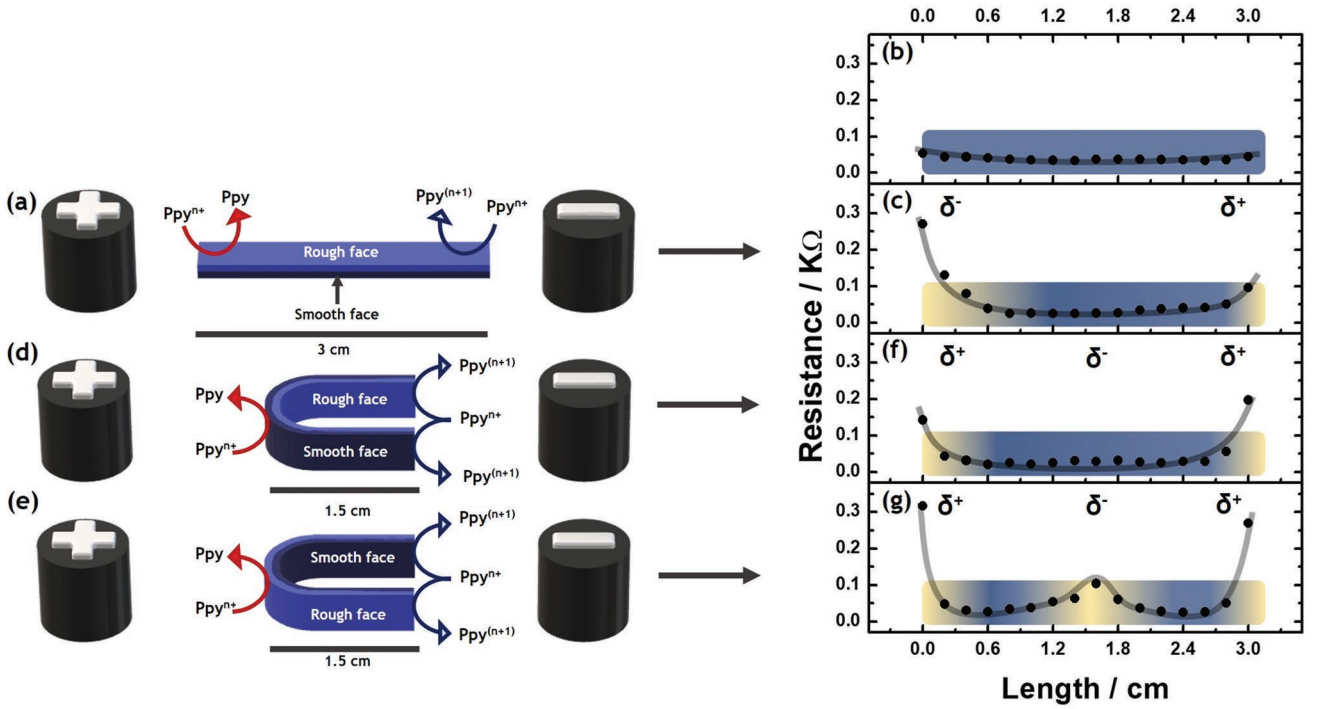

Figure 1. Schematic illustration of the wireless modification of a charged Ppy/DBS strip placed between two feeder electrodes using different spatial configurations of the BPE; a) unfolded and d,e) U-shaped, with a representation of the associated chemical reactions. Resistance values at different positions along the Ppy/DBS films, for: b) pristine Ppy and the different asymmetrically modified Ppy strips, obtained by applying an electric field of: c) 2 V cm^{-1} and f,g) 4 V cm^{-1}, during 30 s. The different tones of yellow and blue symbolize the insulating and conducting regions of the polymer, respectively.

ance profile, and the smooth face presents a globally higher resistance in comparison with the rough part (Figure S3, Supporting Information). This is caused by the compact polymer structure formed at the surface of the Au electrode during the electropolymerization, which limits the mobility of the charge carriers within the Ppy film. In addition, the overoxidation or reduction reactions on the smooth surface are restricted due to mass transport limitations. As it is well-established, the insulating/conducting transition of π-conjugated polymers is accompanied with an uptake/release of ions.[4,46–47] Thus, the ion transfer is slower at the smooth face (compact structure) in comparison with the rough face. This is further illustrated by electromechanical deformation experiments, and evaluating the angle of bending as a function of time. As it can be seen in Figure S4 (Supporting Information), applying a reduction potential (–0.8 V vs Ag/AgCl) to the free-standing Ppy/DBS film induces a continuous bending, due to a more favorable uptake of cations at the rough face of the film.

In order to corroborate the composition modification associated with the redox reactions, energy-dispersive X-ray spectroscopy mappings (EDX) were carried out at different spatial positions along the Ppy strips after the BE measurements. As stated above, the overoxidation of Ppy leads to the formation of pyrrolinones units along the conjugated backbone, which limits the mobility of the charge carriers. Thus, by evaluating the EDX signal around the emission peak of oxygen (O-kα, 0.53 keV), it is possible to visualize the formation of oxygen gradients at the anodic extremities of each BPE. It is important to highlight that the emission peak of oxygen for the pristine Ppy film is also due to the presence of DBS ions within the polymer matrix. The EDX spectra at different positions along the unfolded Ppy strip show a higher amount of oxygen at the δ^+ extremity of the unfolded device (Figure S5a, Supporting Information), whereas the U-shaped BPE presents three well-defined regions enriched with oxygen (Figure S5b, Supporting Information). The plot of the maximum of the normalized emission peaks of oxygen as a function of the position along the Ppy strip, for the unfolded and the U-shaped films with the rough surface facing outwards, shows well-defined oxygen gradients propagating from the anodic and cathodic regions, following the same tendency than the obtained resistance gradients (**Figure 2** and Figure S6, Supporting Information). The gain of oxygen in the anodic regions is expected, due to the formation of pyrrolinones units, but such an increase at the cathodic parts must be due to an alternative redox process. Since the reduction of Ppy commonly takes place at potentials below –0.5 V Ag/AgCl,[4,46–47] it is possible to assume that during the polarization of the polymeric film an additional reduction takes place, i.e., oxygen reduction. This would lead to a local production of hydroxyl ions, remaining trapped in the polymer matrix, which could explain the increase of oxygen in the cathodic regions of the BPE. In any case, the resistance and oxygen gradients are a straightforward evidence of the localized modification of the physicochemical properties of the conducting substrates.

Finally, we extended this approach to even more complex BPE configurations, in order to generate more sophisticated resistance patterns. Once again, the asymmetric modification of the free-standing Ppy/DBS strips was carried out by

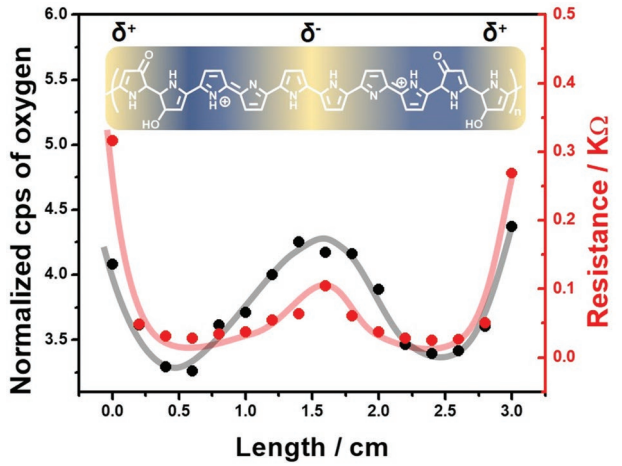

Figure 2. Variations of the maximum normalized emission peaks of oxygen (left axis, black dots) and resistance values (right axis, red dots) at different positions along the Ppy/DBS films, obtained after applying an electric field of 4 V cm^{-1} during 30 s. The different tones of yellow and blue symbolize the insulating and conducting regions of the polymer, respectively.

placing the BPE at the center of a bipolar cell containing a 5-mM $LiClO_4$ aqueous solution. For this set of experiments, two different polymer shapes were used, S- and E-shaped BPEs with an effective length relative to the electric field of 1 and 0.5 cm, respectively (**Figure 3**a,b). Theoretically, in such a configuration, the S- and E-shaped BPEs can produce four and five polarization regions, respectively. However, due to the intrinsic anisotropy in surface roughness of the Ppy film, the modification of the smooth face is restricted. After exposing the S-shaped BPE to a 6 V cm^{-1} electric field for 30 s, the resistance locally changes at three different regions of the Ppy strip (Figure 3c,d).

Due to the spatial arrangement of the BPE in the electrochemical cell, these high resistance regions correspond to one reduction and two overoxidation reactions of the Ppy substrate. In the case of the E-shaped BPE, five high resistance regions should be theoretically produced after the wireless polarization caused by applying a constant ε (12 V cm^{-1}) (Figure 3e). As expected, no significant resistance changes were obtained in the region where the smooth face of the BPE was polarized by the electric field. The remaining four high resistance areas are attributed to two reductions and two overoxidation reactions of the charged Ppy. All the generated resistance gradients propagate locally from the anodic and cathodic regions along the Ppy strip.

3. Conclusion

In conclusion, we have demonstrated the possible generation of localized resistance gradient patterns by bipolar electrochemistry at predictable positions. Such resistance changes are caused by the formation of neutral Ppy and pyrrolinone regions at different locations along the charged Ppy/DBS films. Different BPE with sophisticated spatial configurations were designed by taking advantage of the outstanding mechanical properties of Ppy. The synergy between the flexible conducting substrate and the wireless polarization enables the generation of well-defined resistance gradients. EDX measurements confirmed the localized physicochemical modification, due to changes of the amount of oxygen in the anodic and cathodic regions of the substrate. In all the cases, the formed resistance gradients propagate locally from the anodic and cathodic regions along the Ppy strip. The described approach presents different advantages in comparison with conventional pattering methods, such as the wireless nature of BE and the possible fine-tuning of localized resistance gradients by controlling the

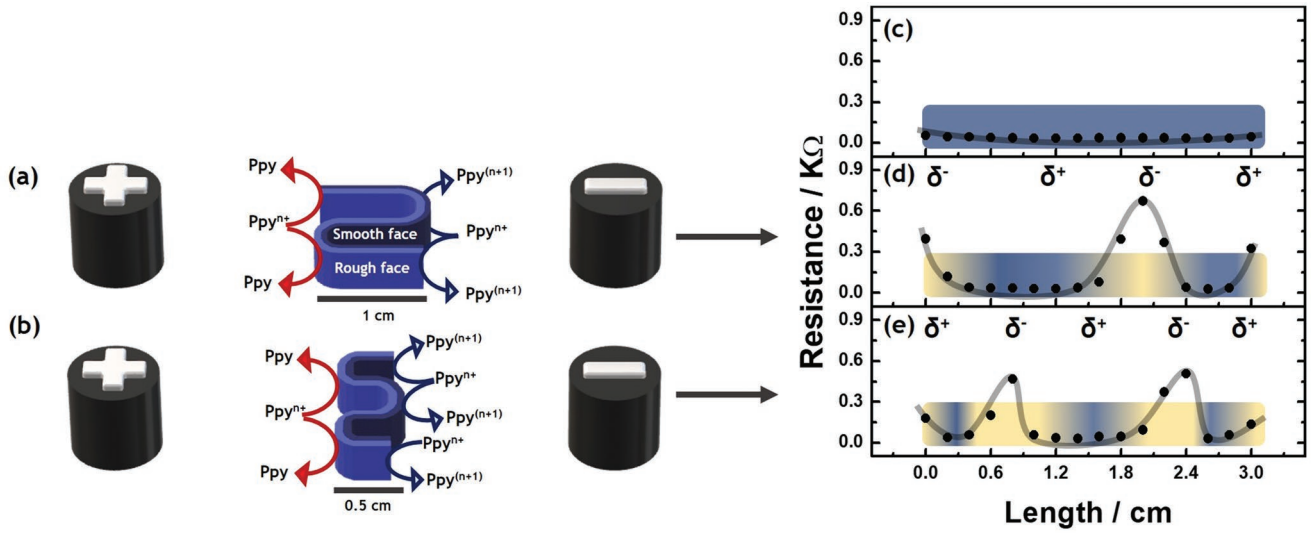

Figure 3. Schematic illustration of the wireless modification of a charged Ppy/DBS strip placed between two feeder electrodes using different spatial configurations of the BPE. a) S- and b) E-shaped polymer, with a representation of the associated chemical reactions. Resistance values at different positions along the Ppy/DBS films, for: c) the pristine Ppy and the different asymmetrical modified Ppy strips, obtained by applying an electric field of: d) 6 V cm^{-1} and e) 12 V cm^{-1}, during 30 s. The different tones of yellow and blue symbolize the insulating and conducting regions of the polymer, respectively.

applied electric field, the experimental time, and the initial shape of the BPE. The three different shapes, which were used in the described experiments, are intended to illustrate that in principle complex conductivity patterns can be designed by following the proposed approach. Pushing the concept further, one could for example imagine to use a kind of polymer "origami," with a much more complex folding, as a bipolar electrode with a certain orientation in the electric field, and thus create sophisticated resistance patterns, desirable for microelectronic devices. The described method can be extended to other conducting polymers and might find so far unexplored applications. For example, since actuation of conducting polymers is based on an asymmetric ion exchange, associated to the redox state of the polymer, leading to swelling and shrinking, the possibility to generate localized resistance spots, can allow the design of actuators with a far more complex dynamic behavior.

4. Experimental Section

Electrochemical Polymerization of Ppy/DBS: The Ppy film was synthesized according to previous reports with a slight modification. Briefly, the galvanostatic polymerization was carried out in an aqueous solution of sodium dodecyl benzenesulfonate (0.25 M, Sigma-Aldrich) and pyrrole monomer (0.2 M, Sigma-Aldrich), by applying a constant current of 8 mA for 1.5 h. Two gold-coated glass slides were positioned parallel in a beaker, filled with 24 cm^3 of this solution. These gold-coated glass slides were used as a working and counter electrode, whereas Ag/AgCl (3 M KCl) was the reference electrode. After polymerization, the Ppy film was washed with water, dried, and peeled off from the substrate.

Wireless Asymmetric Modification: The asymmetric modification was performed by applying a constant electric field for 30 s. The duration was optimized, considering that below 30 s only small changes of resistance were obtained, whereas for too long times, the generated resistance gradients extended over a too large area (Figure S1, Supporting Information). The pristine Ppy strips (0.5 cm × 3 cm) were placed in the center of a bipolar cell containing 15 cm^3 of a 5-mM $LiClO_4$ aqueous solution, used as supporting electrolyte. Two graphite feeder electrodes were positioned at the extremities of the cell (5 cm apart).

Polypyrrole Resistance Measurements: The resistance of the Ppy/DBS films was measured by means of a digital multimeter. Resistance measurements were generally carried out on the rough face of the film, before and after the wireless asymmetric polarization of the polymer, in 16 different regions along the Ppy film, separated from each other by ≈0.2 cm.

Electromechanical Experiments: The actuation measurements were carried out in a three-electrode cell containing a 0.1-M $LiClO_4$ solution, with a pristine free-standing Ppy/DBS film acting as working electrode and a Pt mesh and Ag/AgCl as counter and reference electrode, respectively. The potentiostatic measurements were performed by applying a reduction potential of –0.8 V versus Ag/AgCl for 10 s. The dynamic behavior of the freestanding actuator was monitored by using a CCD camera (CANON EOS 70D, Objective Canon Macro Lens 100 mm 1:2.8). Video processing and tracking was performed with ImageJ software.

SEM and EDX Characterization: Scanning electron microscopy experiments, together with energy-dispersive X-ray spectroscopy mappings were carried out on the rough face of the Ppy film using a Vega3 Tescan 20.0 kV microscope.

Supporting Information

Supporting Information is available from the Wiley Online Library or from the author.

Acknowledgements

The work was funded by the European Research Council under the European Union's Horizon 2020 research and innovation program (grant No. 741251, European Research Council Advanced Grant ELECTRA).

Conflict of Interest

The authors declare no conflict of interest.

Data Availability Statement

The data that support the findings of this study are available from the corresponding author upon reasonable request.

Keywords

bipolar electrochemistry, conducting polymers, resistance gradients, surface modification

Received: November 18, 2022
Revised: January 30, 2023
Published online: March 22, 2023

[1] J. Heinze, B. A. Frontana-Uribe, S. Ludwigs, *Chem. Rev.* **2010**, *110*, 4724.
[2] G. Salinas, B. A. Frontana-Uribe, *ChemElectroChem* **2019**, *6*, 4105.
[3] I. Bargigia, L. R. Savagian, A. M. Osterholm, J. R. Reynolds, C. Silva, *J. Am. Chem. Soc.* **2021**, *143*, 294.
[4] T. F. Otero, J. G. Martinez, *Adv. Funct. Mater.* **2013**, *23*, 404.
[5] B. Roschning, J. Weissmüller, *Adv. Mater. Interfaces* **2020**, *7*, 2001415.
[6] J. G. Ibanez, M. E. Rincon, S. Gutierrez-Granados, M. Chahma, O. A. Jaramillo-Quintero, B. A. Frontana-Uribe, *Chem. Rev.* **2018**, *118*, 4731.
[7] B. Lakard, *Appl. Sci.* **2020**, *10*, 6614.
[8] J. J. Alcaraz-Espinoza, G. Ramos-Sanchez, J. H. Sierra-Uribe, I. Gonzalez, *ACS Appl. Energy Mater.* **2021**, *4*, 9099.
[9] G. Salinas, B. A. Frontana-Uribe, *Electrochem* **2022**, *3*, 492.
[10] B. D. Paulsen, K. Tybrandt, E. Stavrinidou, J. Rivnay, *Nat. Mater.* **2020**, *19*, 13.
[11] Z. Peng, C. Wang, Z. Zhang, W. Zhong, *Adv. Mater. Interfaces* **2019**, *6*, 1901393.
[12] T. Wang, Y. Bao, M. Zhuang, J. Ji, J. Chen, H. Xu, *Nano Res.* **2021**, *14*, 3112.
[13] M. Angelopoulos, *IBM J. Res. Dev.* **2011**, *45*, 57.
[14] J. Park, G. Kim, B. Lee, S. Lee, P. Woo, H. Yoon, H. Cho, S. H. Ko, Y. Hong, *Adv. Mater. Technol.* **2020**, *5*, 2000042.
[15] Z. Su, Z. I. Bedolla-Valdez, L. Wang, Y. Rho, S. Chen, G. Gonel, E. N. Taurone, A. J. Moule, C. P. Grigoropoulos, *ACS Appl. Mater. Interfaces* **2019**, *11*, 41717.
[16] H. Yuk, B. Lu, S. Lin, K. Qu, J. Xu, J. Luo, X. Zhao, *Nat. Commun.* **2020**, *11*, 1604.
[17] Y. Jiang, N. Tang, C. Zhou, Z. Han, H. Qu, X. Duan, *Nanoscale* **2018**, *10*, 20578.
[18] J. Ahn, S. Kwon, S. Jung, W. S. Lee, J. Jeong, H. Lim, Y. B. Shin, J. Lee, *Adv. Mater. Interfaces* **2018**, *5*, 1701593.
[19] N. M. Bojanowski, C. Huck, L. Veith, K. P. Strunk, R. Bäuerle, C. Melzer, J. Freudenberg, I. Wacker, R. Schröder, P. Tegeder, U. H. F. Bunz, *Chem. Sci.* **2022**, *13*, 7880.

[20] M. Mahmoodian, H. Hajihoseini, S. Mohajerzadeh, M. Fathipour, *Synth. Met.* **2019**, *249*, 14.
[21] R. Abargues, P. J. Rodriguez-Canto, R. Garcia-alzada, J. Martinez-Pastor, *J. Phys. Chem. C* **2012**, *116*, 17547.
[22] S. E. Fosdick, K. N. Knust, K. Scida, R. M. Crooks, *Angew. Chem., Int. Ed.* **2013**, *52*, 10438.
[23] L. Koefoed, S. U. Pedersen, K. Daasbjerg, *Curr. Opin. Electrochem.* **2017**, *2*, 13.
[24] L. Bouffier, D. Zigah, N. Sojic, A. Kuhn, in *Encyclopedia of Electrochemistry*, (Ed: A. J. Bard) Wiley, Wiley-VCH Verlag, Weinheim **2022**, https://doi.org/10.1002/9783527610426.bard030112.
[25] N. Shida, Y. Zhou, S. Inagi, *Acc. Chem. Res.* **2019**, *52*, 2598.
[26] K. L. Rahn, R. K. Anand, *Anal. Chem.* **2021**, *93*, 103.
[27] G. Salinas, S. Arnaboldi, L. Bouffier, A. Kuhn, *ChemElectroChem* **2022**, *9*, 202101234.
[28] H. Termebaf, M. Shayan, A. Kiani, *Langmuir* **2015**, *31*, 13238.
[29] S. Ramakrishnan, C. Shannon, *Langmuir* **2010**, *26*, 4602.
[30] C. Ulrich, O. Andersson, L. Nyholm, F. Björefors, *Angew. Chem., Int. Ed.* **2008**, *47*, 3034.
[31] Y. U. Kayran, V. Eβmann, S. Grützke, W. Schuhmann, *ChemElectroChem* **2016**, *3*, 399.
[32] L. Bouffier, S. Reculusa, V. Ravaine, A. Kuhn, *ChemPhysChem* **2017**, *18*, 2637.
[33] L. Fuentes-Rodriguez, E. Pujades, J. Frexedas, A. Crespi, K. Xu, L. Abad, N. Casñ-Pastor, *Mater. Chem. Front.* **2022**, *6*, 2284.
[34] Y. Zhou, N. Shida, I. Tomita, S. Inagi, *Angew. Chem., Int. Ed.* **2021**, *133*, 14741.
[35] L. Koefoed, K. Shimizu, S. U. Pedersen, K. Daasbjerg, A. Kuhn, D. Zigah, *RSC Adv.* **2016**, *6*, 3882.
[36] M. R. Madsen, L. Koedoed, H. Jensen, K. Daasbjerg, S. U. Pedersen, *Electrochim. Acta* **2019**, *317*, 61.
[37] S. Inagi, *Polym. J.* **2016**, *48*, 39.
[38] S. Inagi, Y. Ishiguro, M. Atobe, T. Fuchigami, *Angew. Chem., Int. Ed.* **2010**, *49*, 10136.
[39] Y. Ishiguro, S. Inagi, T. Fuchigami, *Langmuir* **2011**, *27*, 7158.
[40] N. Shida, Y. Ishiguro, M. Atobe, T. Fuchigami, S. Inagi, *ACS Macro Lett.* **2012**, *1*, 656.
[41] S. Inagi, H. Nagai, I. Tomita, T. Fuchigami, *Angew. Chem., Int. Ed.* **2013**, *52*, 6616.
[42] Y. Ishiguro, S. Inagi, T. Fuchigami, *J. Am. Chem. Soc.* **2012**, *134*, 4034.
[43] Y. Li, R. Qian, *Electrochim. Acta* **2000**, *45*, 1727.
[44] R. Holze, *Polymers* **2022**, *14*, 1584.
[45] B. Gupta, B. Goueau, P. Garrigue, A. Kuhn, *Adv. Funct. Mater.* **2018**, *28*, 1705825.
[46] T. F. Otero, J. G. Martinez, *Adv. Funct. Mater.* **2014**, *24*, 1259.
[47] T. F. Otero, L. X. Martinez-Soria, J. Schumacher, L. Valero, V. H. Pascual, *ChemistryOpen* **2017**, *6*, 25.